Posture stabilization of a 3-link nonholonomic manipulator – two control approaches*

Krzysztof Kozłowski, Maciej Michałek, Dariusz Pazderski

Chair of Control and Systems Engineering, Poznań University of Technology, Piotrowo 3a, 60-965 Poznań
email: name.surname@.put.poznan.pl

Abstract *The paper presents two different control approaches, which allow to solve difficult posture stabilization task for a* $3-$*link nonholonomic planar manipulator. Difficulties arise from nonintegrable motion constraints imposed on a system evolution and less number of control inputs in comparison to a state dimension. Presented solutions belong to one of two general stabilization approaches: time-varying or discontinuous one. Control performances of both stabilization strategies have been illustrated by simulation results.*

1. Introduction. The underactuated mechanical systems with nonintegrable motion constraints (nonholonomic contraints) play a very important role in many practical applications. Over two last decades in a robotics literature much work has been devoted to restricted mobility wheeled robots with nonholonomic constraints. Recently, some authors have considered other examples of underactuated robotic system, namely so-called nonholonomic manipulator. It can be regarded as a very interesting solution combining good manipulability properties and lightness of the construction, since number of motors is considerably less than number of independent active joints. However, because of some technical difficulties, not many constructions of nonholonomic manipulators were built so far. One well-known example of such system, which was constructed and experimentally tested uses nonholonomic ball-gears [13, 11]. These gears, mounted in each manipulator joint, play a crucial role in input velocities transmission along the whole kinematic chain. Apart from difficulties in realizing nonholonomic manipulators, very important and challenging is a control problem of such devices. Since nonholonomic manipulator is subjected to nonintegrable constraints, its kinematics can be modeled as an underactuated nonlinear driftless affine system, for which sufficient Brockett's conditions for smooth stabilizability are not met [3]. As a consequence, no continuously differentiable, statically state dependent control law can be used for posture (point) stabilization. Many different strategies to solve the difficult stabilization task were proposed – compare for example [10, 7]. Among them, two major classes of control schemes may be distinguished: time-varying strategies and time-invariant noncontinuous techniques.

In this paper two different approaches of posture stabilization of 3-link nonholonomic manipulator with ball-gears [13, 11] will be presented. The first controller, which may be classified as Time-Varying Oscillatory-based (TVO) stabilizer, is based on a new idea of stabilization initially proposed by Dixon *et al.* [4], and next significantly extended by Morin *et al.* [9]. The time-differentiable control law developed here ensures practical stabilization in the sense, that a regulation error is decreased to the assumed neighborhood of a reference point.

The second considered controller comes from the Vector Field Orientation (VFO) approach introduced for the first time in [5]. The VFO approach results from a simple geometrical interpretation of a controlled kinematic structure and its possible time evolution in a response to specific inputs. The VFO methodology for a non-

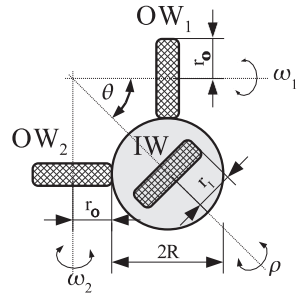

Figure 1. The nonholonomic ball-gear.

holonomic manipulator will be described, and a VFO (C^0 continuous, time-invariant) stabilizer ensuring asymptotic stability will be derived.

The paper is organized as follows. In Section 2 model description of a nonholonomic manipulator equipped with ball-gears is presented. Section 3 is devoted to derivation of two alternative control laws used later for posture stabilization. In the Section 4 simulation results are presented. Concluding remarks are given in Section 5.

2. Kinematics. Nonholonomic manipulator constitutes a very interesting proposition of a new mechanical solution, where $N-$link chain can be driven by only two input signals preserving full controllability of a system in a whole configuration space [13, 11]. The main idea of this solution lies in velocity transmission along manipulator arm, in which nonholonomic ball-gears have been designed and located at particular joints (see Fig.1). Each ball-gear consists of a ball and three wheels rolling on it without slippage. Inputs of the ball-gear are input-wheel (IW) velocity, ρ, and the angular velocity, $\dot{\theta}$, which orients the input-wheel in relation to the ball and two perpendicular output-wheels (OW_1, OW_2). Driving the input-wheel and changing its orientation with respect to output-wheels, one can divide an input-wheel velocity onto two angular velocities of output-wheels as follows:

$$\omega_1 = \rho \frac{r_I}{r_O} \cos\theta, \tag{1}$$

$$\omega_2 = \rho \frac{r_I}{r_O} \sin\theta, \tag{2}$$

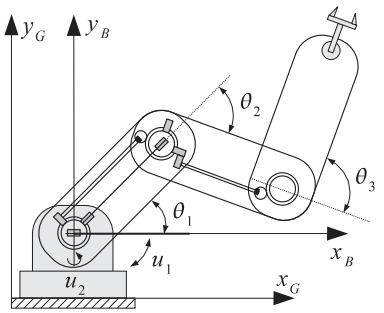

Figure 2. The nonholonomic planar manipulator with three links and two control inputs.

where $\frac{r_I}{r_O}$ describes the ball-gear ratio. Although such a mechanical solution presents many practical benefits, stabilization control task for this system becomes quite difficult due to the Brockett's conditions [3]. Assuming unit ratios of all existing gears, the kinematic model of the 3-link nonholonomic manipulator with particular joint velocity transmission depicted in Fig. 2 can be described as follows:

$$\begin{bmatrix} \dot{\theta}_1 \\ \dot{\theta}_2 \\ \dot{\theta}_3 \end{bmatrix} = \begin{bmatrix} 1 \\ 0 \\ 0 \end{bmatrix} u_1 + \begin{bmatrix} 0 \\ \sin\theta_1 \\ \cos\theta_1 \cos\theta_2 \end{bmatrix} u_2, \tag{3}$$

where $\boldsymbol{q} \triangleq [q_1\ q_2\ q_3]^T \triangleq [\theta_1\ \theta_2\ \theta_3]^T \in \mathcal{Q} \subset \mathbb{R}^3$ is a state vector (configuration angles of a kinematic chain), $u_1, u_2 \in \mathcal{U} \subset \mathbb{R}$ are input signals. Model (3) belongs to a class of nonholonomic driftless systems described in the following general form:

$$\dot{\boldsymbol{q}} = \boldsymbol{g}_1 u_1 + \boldsymbol{g}_2(\boldsymbol{q}) u_2, \tag{4}$$

where $\boldsymbol{g}_1, \boldsymbol{g}_2(\boldsymbol{q})$ are basic vector fields – generators. Nonintegrable velocity constraints obtained directly from equation (3) can be written in Pfaffian form:

$$\boldsymbol{A}(\boldsymbol{q})\dot{\boldsymbol{q}} = \begin{bmatrix} 0 \\ -\cos\theta_2 \cos\theta_1 \\ \sin\theta_1 \end{bmatrix}^T \begin{bmatrix} \dot{\theta}_1 \\ \dot{\theta}_2 \\ \dot{\theta}_3 \end{bmatrix} = 0, \tag{5}$$

where $\boldsymbol{A}(\boldsymbol{q})$ is the constraint matrix. Constraint (5) results from the rolling without slippage assumption in the nonholonomic ball-gear. System (3) is fully controllable in a whole configuration

space $\mathcal{Q} \subset \mathbb{R}^3$, however not all generalized velocities $\dot{\boldsymbol{q}}$ are accessible during its time evolution due to imposed constraints (5). This fact causes, that control tasks become a challenge for control researchers.

The form of the second generator $\boldsymbol{g}_2(\boldsymbol{q})$ in (3) implies, that for some set of configuration points $\mathcal{Q}_s \subset \mathcal{Q}$:

$$\mathcal{Q}_s = \left\{ \boldsymbol{q} : \theta_1 = n\pi \ \wedge \ \theta_2 = (2n-1)\frac{\pi}{2} \right\}_{n=0,\pm 1 \ldots} \tag{6}$$

the vector field $\boldsymbol{g}_2(\boldsymbol{q})$ degenerates to zero. This effect can cause difficulties during stabilization process considered here. Hence, the set of non-regular points $\mathcal{Q}_s$ in the configuration space $\mathcal{Q}$ should be avoided during a control process. For our purposes we exclude some points from the configuration domain and postulate the following assumption:

$$\forall_{\tau \geqslant 0} \quad \theta_2(\tau) \in \left(-\frac{\pi}{2}, \frac{\pi}{2} \right), \tag{7}$$

which guarantees avoiding points from the set $\mathcal{Q}_s$ (see (6)).

3. Posture stabilization. In this paper posture stabilization task for the 3-link nonholonomic manipulator will be considered. In order to determine posture error the following vector $\boldsymbol{e} \in \mathbb{R}^3$ is defined

$$\boldsymbol{e} \triangleq \begin{bmatrix} e_1 \\ e_2 \\ e_3 \end{bmatrix} \triangleq \boldsymbol{q}_t - \boldsymbol{q} = \begin{bmatrix} \theta_{1t} - \theta_1 \\ \theta_{2t} - \theta_2 \\ \theta_{3t} - \theta_3 \end{bmatrix}, \tag{8}$$

where $\boldsymbol{q}_t$ and $\boldsymbol{q}$ determine the reference and actual configuration, respectively. Without lack of generality we assume that the reference point to be stabilized is the origin: $\boldsymbol{q}_t \triangleq [0 \ 0 \ 0]^T$. In the sequel of this paper two control approaches will be described, which allow to solve practical and asymptotic stabilization task for nonholonomic kinematics (3). The practical stabilization task is defined as follows.

Definition 1 *Find bounded controls u_1, u_2 for kinematics (3) such, that Euclidean norm of the stabilization error (8) tends to some neighborhood of zero in the sense, that $\lim_{\tau \to \infty} \|\boldsymbol{e}\| = \varepsilon$, where constant $\varepsilon > 0$ can be made arbitrary small.*

For asymptotic stabilization task it is sufficient to assume in Definition 1 that $\varepsilon = 0$. Therefore, the asymptotic stabilization can be seen as a particular case of practical stabilization.

3.1. Practical stabilization. The first control method (TVO) considered here is based on tuned oscillator idea introduced by W. Dixon and others [4]. It should be noted that this approach can be seen as an particular case of more general theory developed by P. Morin and C. Samson [9] taking advantage of so-called transverse functions. The main feature concerning this control scheme lies in virtual periodic signals tracked by state vector of the system.

Model transformation. In this section we present a control law taking advantage of mathematical properties of the system known as Brockett's nonholonomic integrator [3]. This is the driftless nilpotent system for which controllability in a short time is ensured by the first order Lie bracket. The nonholonomic integrator can be written in the following form (compare [4])

$$\begin{aligned} \dot{\boldsymbol{x}}^* &= \boldsymbol{v}, \\ \dot{x}_3 &= \boldsymbol{x}^{*T} \boldsymbol{J} \boldsymbol{v}, \end{aligned} \tag{9}$$

where $\boldsymbol{x} = \begin{bmatrix} x_1 & x_2 & x_3 \end{bmatrix}^T = \begin{bmatrix} \boldsymbol{x}^{*T} & x_3 \end{bmatrix}^T \in \mathbb{R}^3$ is a state vector, $\boldsymbol{v} = \begin{bmatrix} v_1 & v_2 \end{bmatrix}^T \in \mathbb{R}^2$ denotes an input and $\boldsymbol{J} = \begin{bmatrix} 0 & -1 \\ 1 & 0 \end{bmatrix}$ is the skew-symmetric matrix.

In order to transform kinematic equation (3) to the form of nonholonomic integrator the following nonlinear transformation can be considered (see also [13])

$$\boldsymbol{x} \triangleq \boldsymbol{p}(\boldsymbol{q}) \triangleq \begin{bmatrix} q_3 \\ \frac{\tan q_1}{\cos q_2} \\ 2q_2 - q_3 \frac{\tan q_1}{\cos q_2} \end{bmatrix}. \tag{10}$$

The inverse transformation can be obtained as follows

$$\boldsymbol{q} \triangleq \boldsymbol{p}^{-1}(\boldsymbol{x}) = \begin{bmatrix} \arctan\left(x_2 \cos \frac{1}{2}\left(x_1 x_2 + x_3 \right) \right) \\ \frac{1}{2}\left(x_1 x_2 + x_3 \right) \\ x_1 \end{bmatrix}. \tag{11}$$

One can observe that (10) determines a local diffeomorfism which is well defined if

$$\theta_1, \theta_2 \in \left(-n\frac{\pi}{2},\ n\frac{\pi}{2}\right)_{n=1,2,\ldots}. \qquad (12)$$

However, for practical reasons our considerations are limited to the case for which $n = 1$, namely it is assumed that (7) holds and

$$\forall_{\tau \geqslant 0} \quad \theta_1, \in \left(-\frac{\pi}{2},\ \frac{\pi}{2}\right). \qquad (13)$$

According to (10) it is clear that proposed transformation is strictly nonlinear what can be illustrated geometrically – see Fig. 3. In upper part of this figure quarter of sphere in original joint space (in $\theta_1, \theta_2, \theta_3$ coordinates) is depicted. Next, the result of mapping of the part of sphere using (10) is presented in its lower part. As one can see the original space is nonlinearly rescaled (compare maximum values of x_1, x_2 and x_3). Especially it is observed if angles θ_1 and θ_2 are near singular points (i.e. when they approach $\pm\pi/2$).

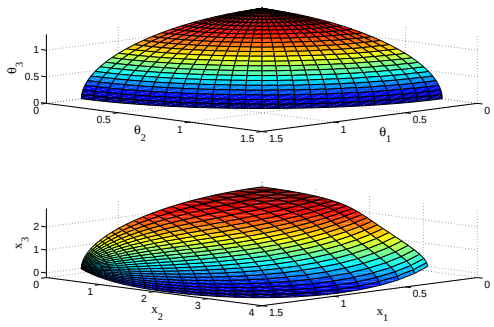

Figure 3. Above: a quarter of the sphere depicted in the joint space (radius of the sphere equals to $\pi/2.5$), below: the mapped quarter of the sphere in auxiliary coordinates

Next, we will make some comments taking into account inverse transformation (11). According to it one can see that for bounded signals x_1, x_2 and $x_3 \in \mathcal{L}_\infty$ coordinate θ_1 is always in the assumed range, i.e. $\theta_1 \in (-\pi/2, \pi/2)$. Proper behavior of θ_3 can be relatively easy ensured since $\theta_3 = x_1$. The main problem is related to the coordinate θ_2 which should satisfy assumption given by (13). However, from (11) it is clear that the inverse transformation cannot guarantee it. Therefore, it is very important to tune the controller in such a way to overcome this obstruction or to switch control strategy if $|x_1 x_2 + x_3| \geqslant \pi$.

Apart from coordinate transformation a relation between original, $\boldsymbol{u}$, and auxiliary, $\boldsymbol{v}$, control signals must be developed. Taking the time derivative of $\boldsymbol{x}^*$ and using (10) one can obtain that

$$\boldsymbol{v} = \boldsymbol{T}(\boldsymbol{q})\,\boldsymbol{u}, \qquad (14)$$

where $\boldsymbol{T}(\boldsymbol{q}) \in \mathbb{R}^{2\times 2}$ is the control transformation matrix defined as

$$\boldsymbol{T}(\boldsymbol{q}) \triangleq \begin{bmatrix} 0 & \cos q_1 \cos q_2 \\ \frac{1}{\cos^2 q_1 \cos q_2} & \frac{\sin q_1}{\cos q_2} \tan q_1 \tan q_2 \end{bmatrix} \qquad (15)$$

with θ_1 and θ_2 satisfying assumptions (7) and (13). Since $\boldsymbol{T}(\boldsymbol{q})$ is invertible as long as (7) and (13) is satisfied, one can obtain that

$$\boldsymbol{u} = \boldsymbol{T}(\boldsymbol{q})^{-1}\,\boldsymbol{v}. \qquad (16)$$

Summarizing, as a result of transformations (10) and (16) it is possible to resolve posture stabilization for the considered nonholonomic manipulator by developing the control law which stabilizes the system given by (9). This approach is presented in the next subsection.

TVO control law. Firstly, for control purpose considered here and taking into account the system (9) the following signal $\boldsymbol{z} \in \mathbb{R}^3$ may be introduced

$$\boldsymbol{z} \triangleq \begin{bmatrix} \boldsymbol{z}^* \\ z_3 \end{bmatrix} = \boldsymbol{x} - \begin{bmatrix} \boldsymbol{x}_d \\ -\boldsymbol{x}_d^T \boldsymbol{J} \boldsymbol{x}^* \end{bmatrix}, \qquad (17)$$

where $\boldsymbol{z}^* = [z_1\ z_2]^T \in \mathbb{R}^2$, $\boldsymbol{x}_d = [x_{d1}\ x_{d2}]^T \in \mathbb{R}^2$ denotes auxiliary time-varying bounded signals which will be defined later.

It should be noted that definition (17) illustrates the main concept of TVO stabilizer as well as other controllers using transverse functions. It consists of decreasing regulation error $\boldsymbol{x}$ indirectly by tracking additional virtual signals $\boldsymbol{x}_d$. Moreover, relation (17) has its roots in differential geometry, since it takes advantage of a left-invariant group operation for system (9) (compare [9, 8]).

The auxiliary task of control consists of asymptotic (exponential) stabilization of $\|\boldsymbol{z}\|$, namely

$$\|\boldsymbol{z}\| \leqslant \gamma \|\boldsymbol{z}(0)\| \exp(-\beta\tau), \tag{18}$$

where $\tau > 0$ denotes time and $\gamma, \beta > 0$ are positive constants.

According to assumption (18) and definition (17) one can conclude that

$$\lim_{\tau\to\infty} \boldsymbol{z}^* = \mathbf{0} \Rightarrow \lim_{\tau\to\infty} \boldsymbol{x}^* = \boldsymbol{x}_d \tag{19}$$

and

$$\lim_{\tau\to\infty} z_3 = 0 \Rightarrow \lim_{\tau\to\infty} x_3 = 0, \tag{20}$$

where $\boldsymbol{x}^* = [x_1 \; x_2]^T$. These relations show that accuracy of regulation in the steady state is determined by signal $\boldsymbol{x}_d$. Moreover, $\boldsymbol{x}_d$ significantly influences the transient states behavior during regulation process since it is tracked by $\boldsymbol{x}^*$ according to (19).

In order to develop the control law which makes $\boldsymbol{z} = \mathbf{0}$ to be asymptotically stable equilibrium point the following Lyapunov candidate function is proposed

$$V = \frac{1}{2}\boldsymbol{z}^T\boldsymbol{z}. \tag{21}$$

Next, taking its one can get

$$\dot{V} = \boldsymbol{z}^T\dot{\boldsymbol{z}} = \boldsymbol{z}^{*T}\dot{\boldsymbol{z}}^* + z_3\dot{z}_3. \tag{22}$$

Calculating the time derivative of $\boldsymbol{z}^*$ from (17) results in

$$\dot{\boldsymbol{z}}^* = \boldsymbol{v} - \dot{\boldsymbol{x}}_d. \tag{23}$$

It should be noted that regulation task concerning vector $\boldsymbol{z}^*$ is relatively easy and can be resolved proposing the following control signal

$$\boldsymbol{v} = -k_1\boldsymbol{z}^* + \dot{\boldsymbol{x}}_d, \tag{24}$$

where $k_1 > 0$ is a controller parameter. Using (24) and (17) in (22) yields in

$$\dot{V} = -k_1\boldsymbol{z}^{*T}\boldsymbol{z}^* + z_3\dot{z}_3. \tag{25}$$

Next, the term $\dot{z}_3$ can be calculated according to (17) as follows

$$\dot{z}_3 = \boldsymbol{x}_d^T\boldsymbol{J}\dot{\boldsymbol{x}}_d + 2k_1\boldsymbol{x}^{*T}\boldsymbol{J}\boldsymbol{x}_d. \tag{26}$$

Here signal $\dot{\boldsymbol{x}}_d$ can be interpreted as an additional control signal and can be used for asymptotic stabilization of coordinate z_3. In order to calculate $\dot{\boldsymbol{x}}_d$ we assume that $\boldsymbol{x}_d$ is originated by tunable oscillator [4] according to the following equation

$$\boldsymbol{x}_d = \boldsymbol{\Psi}\boldsymbol{\xi}, \tag{27}$$

where $\boldsymbol{\Psi} = \begin{bmatrix}\psi_1 & 0\\ 0 & \psi_2\end{bmatrix}$ is a gain matrix with scalar functions $\psi_1(\tau)$ and $\psi_2(\tau) > 0$ which may be changed during regulation process and $\boldsymbol{\xi}$ is a solution of the following differential equation

$$\dot{\boldsymbol{\xi}} = u_\omega\boldsymbol{J}\boldsymbol{\xi} \tag{28}$$

with u_ω determining an instantaneous frequency of $\boldsymbol{\xi}$ and initial condition

$$\boldsymbol{\xi}(0)^T\boldsymbol{\xi}(0) = 1. \tag{29}$$

As one can see (28) describes an undumped linear oscillator with constant amplitude of signal $\boldsymbol{\xi}$, such that $\forall_{\tau>0}\ \boldsymbol{\xi}^T(\tau)\boldsymbol{\xi}(\tau) = 1$. Similarly to the control law given by P. Morin and C. Samson [9] frequency u_ω can be regarded as the third control signal (apart from v_1 and v_2) that makes the system to be virtually fully actuated.

An analytical formula describing u_ω can be obtained using the time derivative of (27), namely

$$\dot{\boldsymbol{x}}_d = \dot{\boldsymbol{\Psi}}\boldsymbol{\xi} + \boldsymbol{\Psi}\dot{\boldsymbol{\xi}} \tag{30}$$

and relations (26) and (24). A a result the following relation can be written

$$\dot{z}_3 = \boldsymbol{\xi}^T\boldsymbol{\Psi}^T\boldsymbol{J}\dot{\boldsymbol{\Psi}}\boldsymbol{\xi} + 2k_1\boldsymbol{x}^{*T}\boldsymbol{J}\boldsymbol{x}_d - \psi_1\psi_2 u_\omega. \tag{31}$$

Then it is straightforward to show that applying u_ω written as

$$u_\omega = \frac{-w + \boldsymbol{\xi}^T\boldsymbol{\Psi}^T\boldsymbol{J}\dot{\boldsymbol{\Psi}}\boldsymbol{\xi} + 2k_1\boldsymbol{x}^{*T}\boldsymbol{J}\boldsymbol{x}_d}{\psi_1\psi_2}. \tag{32}$$

in (31) leads to decoupled subsystem, namely $\dot{z}_3 = w$, where w is a scalar function which is a new input. In order to ensure exponential stabilization of z_3 we propose to set

$$w = -k_2 z_3, \tag{33}$$

where $k_2 > 0$ is a constant controller parameter. Consequently, taking into account (33) allows to rewrite the time derivative of V as

$$\forall_{\tau>0,\|\boldsymbol{z}\|\neq 0}\ \dot{V} = -k_1 \boldsymbol{z}^{*T}\boldsymbol{z}^* - k_2 z_3^2 < 0. \quad (34)$$

Then, assuming that $\beta = \min\{k_1, k_2\}$ the following upper bound of $\dot{V}$ can be written

$$\dot{V} \leqslant -\beta \boldsymbol{z}^T\boldsymbol{z} = -2\beta V. \quad (35)$$

As a consequence one can prove that V tends to zero exponentially, namely

$$\forall_{\tau>0}\ V(\tau) = V(0)\exp(-2\beta\tau). \quad (36)$$

Proposition 1 *Assuming that k_1, k_2, ψ_1 and $\psi_2 > 0$ and ψ_1, ψ_2, $\dot{\psi}_1$ and $\dot{\psi}_2 \in \mathcal{L}_\infty$, the controller given by (24), (32), (33), (27), (28) and (29) stabilizes the system (17) exponentially in the sense given by (18).*

Considering (32) one can see that frequency of oscillation u_ω is strictly related to functions ψ_1 and ψ_2 determining amplitude of auxiliary signal $\boldsymbol{x}_d$. In the case when $\|\boldsymbol{z}\|$ is high with respect to ψ_1 and ψ_2 high frequency of oscillation will appear. Hence, choosing ψ_1 and ψ_2 properly is very important since it may improve transient behavior of the controlled system. On the other hand $\boldsymbol{x}_d$ determines an accuracy of regulation in the steady-state, according to relation (19). Therefore it is reasonable to assume that at the beginning of regulation process values of ψ_1 and ψ_2 should be chosen high enough so they tend to small values as time goes to infinity. Similarly to [4] the following proposition regarding ψ_1 and ψ_2 may be assumed

$$\psi_i(\tau) = \psi_{i0}\exp(-\alpha_i\tau) + \varepsilon_i,\ \text{for } i = 1, 2, \quad (37)$$

where $\psi_{i0} > 0$, $\alpha_i > 0$ and $\varepsilon_i > 0$ are scalar coefficients determining initial and limit value of functions ψ_i and their convergence rate, respectively.

Then using the scaling functions given by (37) one can prove according to (19) and (20) that

$$\lim_{\tau\to\infty}\begin{cases} |x_1| \leqslant \varepsilon_1 \\ |x_2| \leqslant \varepsilon_2 \\ x_3 = 0. \end{cases} \quad (38)$$

Finally, we return to the stabilization problem of nonholonomic manipulator in joint space. According to errors given by (8) and transformation (11) one can conclude that $\lim_{\tau\to\infty} \boldsymbol{x} = \boldsymbol{0}$ implies $\lim_{\tau\to\infty} \boldsymbol{e} = \boldsymbol{0}$. As a result the following proposition can be formulated.

Proposition 2 *Assuming that $\boldsymbol{q}$ satisfy assumption (13) the controller given by (24), (32), (27), (28), (29) and (37) with transformations (10) and (16) ensures boundnesses of the errors $\mathbf{e}$ in the sense given by*

$$\lim_{\tau\to\infty}\begin{cases} |e_1| \leqslant \varepsilon_2 \\ |e_2| \leqslant \frac{1}{2}\varepsilon_1\varepsilon_2 \\ |e_3| \leqslant \varepsilon_1 \end{cases}. \quad (39)$$

Remark 1 *Exponential convergence of an auxiliary error $\boldsymbol{z}$ (see (18)) implies exponential convergence transformed state vector to the set of desired point with size determined by $\boldsymbol{\varepsilon}_i$. Consequently, considering inverse transformation $\boldsymbol{p}^{-1}$ (11) one can make the similar conclusion with respect to error $\mathbf{e}$ convergence. Moreover, the convergence rate can be determined easily, since it is directly related to the selection of k_1, k_2 as well as α_i parameter (compare (36) and (37)).*

Remark 2 *Based on Lyapunov stability analysis it can be observed that the control law given by (24) and (32) may be simplified. According to the simulation results it was observed that the better transient behavior of the system (i.e. less oscillatory) is possible if the time derivatives of ψ_1 and ψ_2 are neglected. Assuming that gains k_1 and k_2 are chosen to be high enough in respect to $\dot{\psi}_1$ and $\dot{\psi}_2$ the modified control law written as*

$$\begin{aligned} \boldsymbol{v} &= -k_1\boldsymbol{z} + \boldsymbol{\Psi}\dot{\boldsymbol{\xi}}, \\ u_\omega &= \frac{k_2 z_3 + 2k_1 \boldsymbol{x}^{*T}\boldsymbol{J}\boldsymbol{x}_d}{\psi_1\psi_2} \end{aligned} \quad (40)$$

makes the point $\boldsymbol{z} = \boldsymbol{0}$ to be asymptotically stable.

3.2. Asymptotic stabilization. In the next section the Vector Field Orientation (VFO) method, which allows to solve the posture stabilization task, will be described. The VFO strategy has been introduced for the first time in [5].

VFO approach. The VFO concept directly comes from a simple and intuitive geometrical interpretation of the structure of controlled kinematics (3) and its possible time evolution in a response to specific controls u_1 and u_2. The main idea involves decomposition of eq. (3) into two subsystems:

$$\dot{\theta}_1 = u_1, \tag{41}$$

$$\begin{bmatrix}\dot{\theta}_2 \\ \dot{\theta}_3\end{bmatrix} = \begin{bmatrix}\sin\theta_1 \\ \cos\theta_1\cos\theta_2\end{bmatrix} u_2 \triangleq \boldsymbol{g}_2^*(\boldsymbol{q})\, u_2. \tag{42}$$

The first 1-D subsystem is linear, the second one (2-D) is nonlinear. One can notice, that the direction of time evolution of state variables θ_2 and θ_3 in $\mathbb{R}^2$ depends on the direction of the vector field $\boldsymbol{g}_2^*(\boldsymbol{q})$:

$$Dir\{\dot{\boldsymbol{q}}^*\} = Dir\{\boldsymbol{g}_2^*(\boldsymbol{q})\}, \tag{43}$$

where $\dot{\boldsymbol{q}}^* \triangleq [\dot{\theta}_2\ \dot{\theta}_3]^T$ and $Dir\{\boldsymbol{z}\}$ denotes the direction of $\boldsymbol{z}$ in space $\mathbb{R}^N$ (here in $\mathbb{R}^2$). Since both components of $\boldsymbol{g}_2^*(\boldsymbol{q})$ depend on the first state variable θ_1, the current direction of $\boldsymbol{g}_2^*(\boldsymbol{q})$ can be changed by changing the actual value of θ_1. From (41) it results, that this change can be accomplished relatively easy with the first input signal u_1. All accessible orientations (and directions) of $\boldsymbol{g}_2^*(\boldsymbol{q})$ in $\mathbb{R}^2$ as a function of variable θ_1 have been depicted in Fig. 4, where variable θ_2 has been assumed to be fixed and equal to $\pi/4$. Since θ_1 directly affects the orientation[1] of $\boldsymbol{g}_2^*(\boldsymbol{q})$, it can be called the *orienting variable*. Next, because input u_1 directly drives the orienting variable θ_1, it can be called the *orienting control*. It is easy to find, that the second input u_2 drives the sub-state $\boldsymbol{q}^* \triangleq [\theta_2\ \theta_3]^T$ along a current direction of $\boldsymbol{g}_2^*(\boldsymbol{q})$. One can say, that u_2 *pushes* the sub-state $\boldsymbol{q}^*$ along this vector field. Hence u_2 will be called the *pushing control*. Aforementioned interpretation and terminology allows to describe the VFO control methodology for system described by eqs. (41) and (42). In order to do that, we have to introduce some additional vector field $\boldsymbol{h}(\tau) \triangleq [h_1(\tau)\ h_2(\tau)\ h_3(\tau)]^T$ which will be called the *convergence vector*. Next we assume, that this vector determines an instantaneous convergence direction (orientation), which should be followed by controlled system to reach the reference goal point $\boldsymbol{q}_t$. At the moment we assume, that $\boldsymbol{h}$ is given. Now the VFO control strategy can be explained as follows. Since $\boldsymbol{h}$ defines the convergence direction, it is desirable to put the direction of generalized velocity vector field $\dot{\boldsymbol{q}}$ of the controlled system (3) onto direction of $\boldsymbol{h}$ with the first input u_1. Simultaneously the subsystem (42) should be pushed along the currently oriented vector field $\dot{\boldsymbol{q}}$ with the second input u_2. Moreover, it seems to be reasonable to push the subsystem (42) only proportionally to a current orthogonal projection of $\boldsymbol{h}^* \triangleq [h_2\ h_3]^T$ onto the instantaneous direction of $\boldsymbol{g}_2^*(\boldsymbol{q})$ (or $\dot{\boldsymbol{q}}^*$ due to (43)). As far as a convergence of θ_1 variable is concerned, the whole vector field $\boldsymbol{h}$ should be designed such as it ensures tending of θ_1 to its reference value at the limit as θ_2 and θ_3 reach their reference values. Mathematically, the VFO strategy can be written in the following form:

$$\textit{find}\ u_1 : \left\{ \lim_{\tau\to\infty} (\dot{\boldsymbol{q}} \parallel \boldsymbol{h}) \Leftrightarrow \lim_{\tau\to\infty} (\dot{\boldsymbol{q}}\, k = \boldsymbol{h}) \right\},$$

$$\textit{find}\ u_2 : \{\ \| \dot{\boldsymbol{q}}^* \| \propto \| \boldsymbol{h}^* \| \cos\alpha \},$$

where $k = k() \neq 0$ is a scalar function and $\alpha\angle(\boldsymbol{g}_2^*(\boldsymbol{q}), \boldsymbol{h}^*)$. According to described strategy, conditions which assure matching directions of two vector fields $\boldsymbol{h}$ and $\dot{\boldsymbol{q}}$ will be derived. The

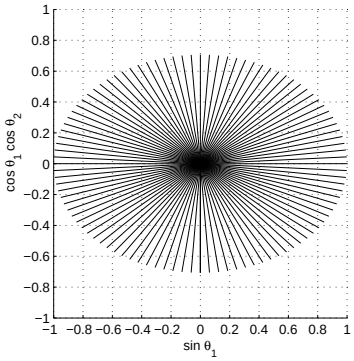

Figure 4. Accessible orientations (and directions) of vector field $\boldsymbol{g}_2^*(\boldsymbol{q})$ (see (42)) in $\mathbb{R}^2$ as a function of orienting variable θ_1 and for fixed $\theta_2 = \pi/4$ (plot with discretization $\Delta\theta_1 = 2\pi/100[rad]$).

[1] Strictly speaking, the *orientation* of some vector field $\boldsymbol{z}$ means its *direction* in $\mathbb{R}^N$ along with its sense.

first of the above relations can be rewritten as follows:

$$u_1 : \lim_{\tau\to\infty} \left\{ \begin{bmatrix} \dot\theta_1 \\ \dot\theta_2 \\ \dot\theta_3 \end{bmatrix} \; k = \begin{bmatrix} h_1 \\ h_2 \\ h_3 \end{bmatrix} \right\} \overset{(3)}{\Rightarrow}$$

$$\overset{(3)}{\Rightarrow} \lim_{\tau\to\infty} \left\{ \begin{bmatrix} u_1\, k \\ \sin\theta_1 u_2\, k \\ \cos\theta_1 \cos\theta_2 u_2\, k \end{bmatrix} = \begin{bmatrix} h_1 \\ h_2 \\ h_3 \end{bmatrix} \right\}.$$

Combining the last two relations one can obtain two so called *VFO orienting conditions*:

$$\textit{find } u_1 : \lim_{\tau\to\infty} \left\{ \begin{array}{c} u_1\, k() = h_1 \\ \tan\theta_1 = \frac{k() h_2 \cos\theta_2}{k() h_3} \end{array} \right\}. \quad (44)$$

These conditions should be met to ensure putting direction of $\dot{\boldsymbol{q}}$ onto direction of $\boldsymbol{h}$ and will be directly used in the next section for design purposes of the first control signal u_1. Function $k()$, which appears in these conditions is not needed to be known explicitly[2], but its sign will be helpful to properly shape the transient states of the whole control system. Let us assume, that the following equality holds: $sgn(k()) = sgn(e_{30})$, where e_{30} denotes the initial value of the stabilization error $e_3 = \theta_{3t} - \theta_3$.

VFO control law. The first relation in (44) can be fulfilled instantaneously by proper definition of signal u_1. But the second one can be generally met only at the limit as $\tau \to \infty$. Hence, let us introduce the *auxiliary direction variable*:

$$\theta_{1d} \overset{\Delta}{=} \text{Atan2}\left(sgn(e_{30}) h_2 \cos\theta_2, sgn(e_{30}) h_3\right) \quad (45)$$

and the *auxiliary error*:

$$e_{1d} \overset{\Delta}{=} \theta_{1d} - \theta_1, \quad (46)$$

where $\text{Atan2}\,(.,.)$ denotes the four-quadrant inverse tangent function and:

$$sgn(z) \overset{\Delta}{=} \left\{ \begin{array}{rll} 1\,, & \text{for} & z \geqslant 0, \\ -1\,, & \text{for} & z < 0. \end{array} \right. \quad (47)$$

Now, to fulfill the second condition in (44) it suffices to guarantee, that the error e_{1d} tends to zero. Therefore, we propose to define the first component of the convergence vector as follows:

$$h_1 \overset{\Delta}{=} k()[k_1 e_{1d} + \dot\theta_{1d}], \quad (48)$$

where $k_1 > 0$ is a design coefficient and feedforward term can be computed as follows

$$\dot\theta_{1d} \overset{(45)}{=} \frac{(\dot h_2 h_3 - h_2 \dot h_3)\cos\theta_2 - h_2 h_3 \dot\theta_2 \sin\theta_2}{h_3^2 + h_2^2 \cos^2\theta_2}. \quad (49)$$

Finally, to meet the first relation in (44), it suffices to take:

$$u_1 \overset{\Delta}{=} \frac{h_1}{k()} \overset{(48)}{=} k_1 e_{1d} + \dot\theta_{1d}. \quad (50)$$

The control law given by (50) guarantees, that: $\lim_{\tau\to\infty} e_{1d} = 0$ (it will be proved in the sequel).

Now, the last two components h_2 and h_3 of a convergence vector $\boldsymbol{h}$ will be defined. Let us introduce the following proposition:

$$\boldsymbol{h}^* = \left[\begin{array}{c} h_2 \\ h_3 \end{array} \right] \overset{\Delta}{=} k_p \boldsymbol{e}^* + \dot{\boldsymbol{q}}^*_{vt}, \quad \boldsymbol{e}^* \overset{\Delta}{=} \left[\begin{array}{c} e_2 \\ e_3 \end{array} \right], \quad (51)$$

where $k_p > 0$ is a design coefficient. The last term $\dot{\boldsymbol{q}}^*_{vt}$ is defined as

$$\dot{\boldsymbol{q}}^*_{vt} \overset{\Delta}{=} -\eta \,\|\,\boldsymbol{e}^*\|\, sgn(e_{30}) \boldsymbol{g}^*_{2t}, \quad 0 < \eta < k_p \quad (52)$$

and is called the *virtual reference velocity*, where:

$$\boldsymbol{g}^*_{2t} = \boldsymbol{g}^*_2(\boldsymbol{q}_t) \overset{(3)}{=} \left[\begin{array}{c} \sin\theta_{1t} \\ \cos\theta_{1t}\cos\theta_{2t} \end{array} \right] = \begin{bmatrix} 0 \\ 1 \end{bmatrix}. \quad (53)$$

Coefficient η allows to shape the transient states. According to VFO strategy it remains to define the pushing control u_2. Following considerations conducted in this subsection, we propose to take:

$$u_2 \overset{\Delta}{=} \frac{1}{\|\,\boldsymbol{g}^*_2\|} \|\,\boldsymbol{h}^*\| \cos\alpha, \qquad \|\,\boldsymbol{g}^*_2\| \neq 0 \quad (54)$$

where $\alpha \angle(\boldsymbol{g}^*_2, \boldsymbol{h})$ and (for $\|\,\boldsymbol{g}^*_2\|, \|\,\boldsymbol{h}^*\| \neq 0$):

$$\cos\alpha \overset{\Delta}{=} \frac{\boldsymbol{g}^{*T}_2 \boldsymbol{h}^*}{\|\,\boldsymbol{g}^*_2\|\,\|\,\boldsymbol{h}^*\|}. \quad (55)$$

Substituting (55) into (54) yields the simpler form of definition of signal u_2:

$$u_2 = \frac{\boldsymbol{g}^{*T}_2 \boldsymbol{h}^*}{\|\,\boldsymbol{g}^*_2\|^2} = \frac{h_2 \sin\theta_1 + h_3 \cos\theta_1 \cos\theta_2}{\sin^2\theta_1 + \cos^2\theta_1 \cos^2\theta_2}. \quad (56)$$

[2] As it will be shown, function $k()$ does nowhere appear in final definitions of control signals.

Recalling assumption (7) it results, that $\forall_{\tau \geqslant 0} \| \boldsymbol{g}_2^* \| \neq 0$ and formulas (54) or (56) are always well defined. Now we can formulate the following proposition.

Proposition 3 *Assuming (7) and conditions:* $\boldsymbol{e}^*(0) \neq \boldsymbol{0}$, $\forall_{\tau<\infty} \| \boldsymbol{h}^* \| \neq 0$, *the VFO controller given by (50) and (56) stabilizes the reference point* $\boldsymbol{q}_t = [0\ 0\ 0]^T$ *in a sense, that* $\lim_{\tau\to\infty} \{\boldsymbol{q}(\tau) \to \boldsymbol{q}_t\}$.

Proof: First, we consider behavior of the auxiliary error e_{1d}. Substituting (50) into (3) yields the following error equation:

$$\dot{e}_{1d} + k_1 e_{1d} = 0 \quad \Rightarrow \quad \lim_{\tau\to\infty} e_{1d} = 0. \quad (57)$$

Hence, the auxiliary error, e_{1d}, exponentially converges to zero as $\tau \to \infty$. Now we will show the convergence of the error $\boldsymbol{e}^*$. For posture stabilization task one can write:

$$\boldsymbol{e}^* \stackrel{\Delta}{=} \boldsymbol{q}_t^* - \boldsymbol{q}^* \quad \Rightarrow \quad \dot{\boldsymbol{e}}^* = -\dot{\boldsymbol{q}}^*. \quad (58)$$

Using (51) one can rewrite the above right hand side equation as follows:

$$\dot{\boldsymbol{e}}^* = -\dot{\boldsymbol{q}}^* + \boldsymbol{h}^* - k_p \boldsymbol{e}^* - \dot{\boldsymbol{q}}_{vt}^*,$$

which can be ordered as follows:

$$\dot{\boldsymbol{e}}^* + k_p \boldsymbol{e}^* = \boldsymbol{r} - \dot{\boldsymbol{q}}_{vt}^*, \qquad \boldsymbol{r} = \boldsymbol{h}^* - \dot{\boldsymbol{q}}^*. \quad (59)$$

Making simple calculations one may derive the following useful relations:

$$\| \boldsymbol{r} \|^2 = \| \boldsymbol{h}^* \|^2 (1 - \cos^2 \alpha), \quad (60)$$

where $\cos\alpha$ is defined by (55) and

$$\lim_{\theta_1 \to \theta_{1d}} (1 - \cos^2 \alpha) = 0. \quad (61)$$

Now we propose to choose the following positive definite Lyapunov function:

$$V(\boldsymbol{e}^*) \stackrel{\Delta}{=} \frac{1}{2} \boldsymbol{e}^{*T} \boldsymbol{e}^* \ . \quad (62)$$

The time derivative of the above function can be estimated as follows (to simplify the notation, we use $\gamma = \sqrt{1 - \cos^2\alpha}$ and $\delta = -\eta \| \boldsymbol{e}^* \| \, sgn(e_{30})$):

$$\begin{aligned}
&\dot{V} = \boldsymbol{e}^{*T} \dot{\boldsymbol{e}}^* \stackrel{(59)}{=} \boldsymbol{e}^{*T} (-k_p \boldsymbol{e}^* + \boldsymbol{r} - \dot{\boldsymbol{q}}_{vt}^*) = \\
&\stackrel{(52)}{=} \boldsymbol{e}^{*T} (-k_p \boldsymbol{e}^* + \boldsymbol{r} - \delta \, \boldsymbol{g}_{2t}^*) = \\
&= -k_p \| \boldsymbol{e}^* \|^2 + \boldsymbol{e}^{*T} \boldsymbol{r} - \delta \boldsymbol{e}^{*T} \boldsymbol{g}_{2t}^* \leqslant \\
&\leqslant -k_p \| \boldsymbol{e}^* \|^2 + \| \boldsymbol{e}^* \| \, \| \boldsymbol{r} \| + |\delta| \, \| \boldsymbol{e}^* \| \, \| \boldsymbol{g}_{2t}^* \| = \\
&\stackrel{(53)}{=} -k_p \| \boldsymbol{e}^* \|^2 + \| \boldsymbol{e}^* \| \, \| \boldsymbol{r} \| + |\delta| \, \| \boldsymbol{e}^* \| = \\
&\stackrel{(60)}{=} -k_p \| \boldsymbol{e}^* \|^2 + \| \boldsymbol{e}^* \| \, \| \boldsymbol{h}^* \| \, \gamma + |\delta| \, \| \boldsymbol{e}^* \| = \\
&\stackrel{(51)}{=} -k_p \| \boldsymbol{e}^* \|^2 + \| \boldsymbol{e}^* \| \, [\, \| \, k_p \boldsymbol{e}^* + \dot{\boldsymbol{q}}_{vt}^* \| \, \gamma + |\delta| \,] \leqslant \\
&\leqslant -k_p \| \boldsymbol{e}^* \|^2 + \| \boldsymbol{e}^* \| \, [\, (k_p \| \boldsymbol{e}^* \| + |\delta|) \gamma + |\delta| \,] = \\
&= -k_p (1 - \gamma) \| \boldsymbol{e}^* \|^2 + |\delta| \, (1 + \gamma) \| \boldsymbol{e}^* \| = \\
&= -[k_p - k_p \gamma - \eta - \eta\gamma] \| \boldsymbol{e}^* \|^2 \ .
\end{aligned}$$

The above time derivative is negative-definite, if the term in brackets is positive. It gives the following convergence condition:

$$\gamma < (k_p - \eta)/(k_p + \eta) \ \Rightarrow \ \lim_{\tau\to\infty} \| \boldsymbol{e}^* \| \to 0. \quad (63)$$

Since $0 < \eta < k_p$ and relations (61) and (57) hold, one concludes:

$$\exists_{\tau_\gamma > 0} \ : \ \forall_{\tau > \tau_\gamma} \quad \gamma < (k_p - \eta)/(k_p + \eta) \quad (64)$$

and the norm $\| \boldsymbol{e}^* \|$ tends asymptotically (exponentially for $\tau > \tau_\gamma$) to zero as $\tau \to \infty$.

Now, it remains to prove convergence of error e_1. Due to (57), it suffices to show, that $\lim_{\tau\to\infty} \theta_{1d} \to 0$. According to definition (45), we have to show, that h_2 component always tends to zero faster than h_3. Recalling (51), (52) we have:

$$\begin{array}{rcl} h_2 & = & k_p e_2, \\ h_3 & = & k_p e_3 - \eta \| \boldsymbol{e}^* \| \, sgn(e_{30}), \end{array} \quad (65)$$

Moreover, it is easy to show that:

$$\lim_{\theta_1 \to \theta_{1d}} \left\{ \begin{array}{l} \dot{\theta}_2 = h_2, \\ \dot{\theta}_3 = h_3. \end{array} \right. \stackrel{(58)}{\Rightarrow} \lim_{\theta_1 \to \theta_{1d}} \left\{ \begin{array}{l} \dot{e}_2 = -h_2, \\ \dot{e}_3 = -h_3. \end{array} \right. \quad (66)$$

Substituting (65) into (66) yields:

$$\lim_{\theta_1 \to \theta_{1d}} \left\{ \begin{array}{rcl} \dot{e}_2 + k_p e_2 & = & 0, \\ \dot{e}_3 + k_p e_3 & = & \eta \| \boldsymbol{e}^* \| \, sgn(e_{30}). \end{array} \right.$$

It is clear, that e_2 tends to zero faster, than e_3. Taking into account (65) it is also clear, that at

the limit $\| \boldsymbol{e}^* \| \to 0$, component $h_2 \to 0$ always faster than h_3. Hence we have shown, that:

$$\lim_{\| \boldsymbol{e}^* \| \to 0} (\theta_{1d} \to 0) \overset{(57)}{\Rightarrow} \lim_{\| \boldsymbol{e}^* \| \to 0} (\theta_1 \to 0).$$

Since h_2, h_3 and $\theta_1 \in \mathcal{L}_\infty$ and if $\forall_{\tau<\infty} \| \boldsymbol{h}^* \| \neq 0$ the feedforward term $\dot{\theta}_{1d} \in \mathcal{L}_\infty$ and recalling (7) one concludes that control signals (50) and (56) are bounded.

□

Remark 3 *Definition (45) is not determined, when the controlled system is at the reference point $\boldsymbol{q}_t^*$, what means $e_2 = e_3 = 0 \Rightarrow h_2 = h_3 = 0$. This indeterminacy can be avoided defining Atan2 $(0,0) \triangleq 0$. With assumption that $\boldsymbol{q}_t$ is the origin, this proposition ensures, that $\boldsymbol{e}^* = \boldsymbol{0} \Rightarrow \theta_{1d} = \theta_{1t} \Rightarrow e_{1d} \equiv e_1$. It should be noted, that the indeterminacy of the type $\theta_{1d} =$ Atan2 $(0,0)$ never occurs if the condition (64) is met. Assuming $\| \boldsymbol{e}^*(0) \| \neq 0$, such indeterminacy could only occur at the limit $\tau \to \infty$, what theoretically means never [2, 1]. Although from a practical point of view and in the case when $\| \boldsymbol{e}^*(0) \| = 0$, determination of θ_{1d} and $\dot{\theta}_{1d}$ at this point is needed. The proposition is to take for $\| \boldsymbol{e}^* \| = 0$: $\theta_{1d} \triangleq 0 = \theta_{1t}$ and $\dot{\theta}_{1d} \triangleq 0$, what allows to use controls (50) and (56) without changes.*

Remark 4 *Fulfilling the conditions: (7) and $\forall_{\tau<\infty} \| \boldsymbol{h}^* \| \neq 0$ during the transient stage depends on the effectiveness of the orienting process – the shorter time interval τ_γ (see (64)), the earlier convergence rate of $\boldsymbol{e}^*$ becomes exponential. Hence to ensure above mentioned conditions during the transient stage, the following strategy can be applied : use the orienting control (50) with $u_2 = 0$ to meet condition (64). Next apply the complete VFO stabilizer (50) and (56) to accomplish the stabilization task ensuring exponential convergence of $\| \boldsymbol{e}^* \|$ to zero.*

4. Simulation results. To show the effectiveness of the proposed stabilization strategies, numerical simulations have been conducted. For both control approaches stabilized reference point has been set to be the origin: $\boldsymbol{q}_t \triangleq [0\ 0\ 0]^T$. Simulations have been carried out within the time horizon $\tau_h = 10[s]$ and for the following initial conditions: $\theta_1(0) = -0.8[rad]$, $\theta_2(0) = 1.2[rad]$ and $\theta_3(0) = 0.5[rad]$.

4.1. TVO stabilizer. The parameters of the controller presented in Section 3.1 have been selected as: $k_1 = k_2 = 6$, $\boldsymbol{\xi}(0) = \frac{1}{\sqrt{2}}[1\ -1]^T$, $\psi_1 = \psi_2 = 1.5$, $\varepsilon_1 = \varepsilon_2 = 10^{-3}$ and $\alpha_1 = \alpha_2 = 2.5$. The simulations have been performed in two cases. In the first case time derivative of $\boldsymbol{\Psi}$ was used while in the second case it was ignored according to simplified version of the controller given by (40).

Based on time plots of regulation errors depicted in Figs. 5 and 6 one can conclude, that neglecting the term $\dot{\boldsymbol{\Psi}}$ allows to improve transient behavior and to reduce oscillations. Convergence rate of the error, $\boldsymbol{e}$, for both TVO controllers are quite similar. In addition, dynamic properties of the simplified control scheme seems to be significantly better. It should be noted, that in both cases singular points in the configuration space are avoided (compare paths in Fig. 8).

Fig. 7 shows both physical, $\boldsymbol{u}$, and virtual, u_ω, control signals. According to it one can see that they are bounded for $\tau > 0$. Relatively high values of $\boldsymbol{u}$ at the beginning of regulation process results from nonlinearity of transformation $\boldsymbol{P}$ (note that $\theta_2(0)$ is quite far from the origin and near a singular point).

4.2. VFO stabilizer. The VFO stabilizer has been tested assuming the following parameter values: $k_1 = 5,\ k_p = 5$ and $\eta = 3$. Since continuous variables $\theta_i(\tau) \in \mathbb{R},\ i = 1, 2, 3$ were not limited to the range $[-\pi, \pi)$, to avoid discontinuity resulting from definition (45), the continuous method of determining (45) has been applied, which is equivalent to the following formula: $\theta_{1d}(\tau) = \theta_{1d}(0) + \int_0^{\tau_h} \dot{\theta}_{1d}(\tau) d\tau$, where $\theta_{1d}(0)$ is computed by (45), $\dot{\theta}_{1d}(\tau)$ is taken from (49) and the integral is computed numerically. As a consequence, the terms θ_{1d} and $e_{1d} \in \mathbb{R}$ are continuous.

Dynamic and static quality can be evaluated comparing Figs. 9-12. From Fig. 9 it can be seen, that convergence of stabilization errors is relatively fast and the error e_2 tends to zero faster

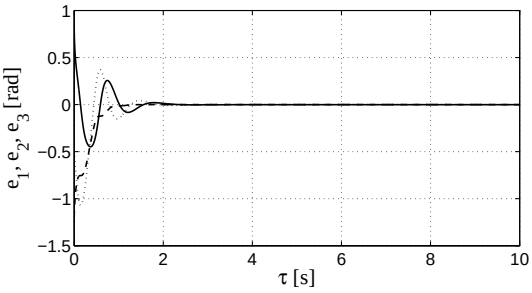

Figure 5. Stabilization errors for original TVO controller: $e_1(\tau)$ (–), $e_2(\tau)$ (- -), $e_3(\tau)$ ($\cdots$).

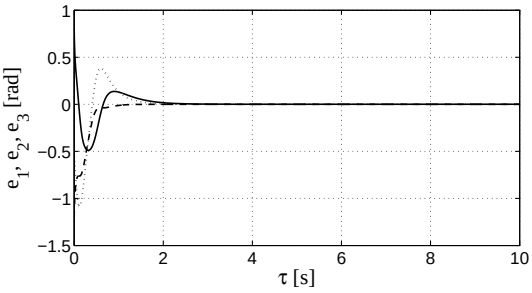

Figure 6. Stabilization errors for simplified TVO controller: $e_1(\tau)$ (–), $e_2(\tau)$ (- -), $e_3(\tau)$ ($\cdots$).

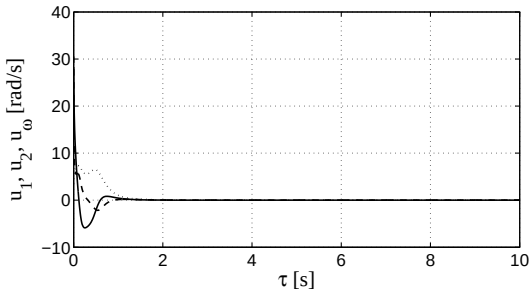

Figure 7. Control signals for simplified TVO controller: $u_1(\tau)$ (- -), $u_2(\tau)$ (–) and $u_\omega(\tau)$ ($\cdots$).

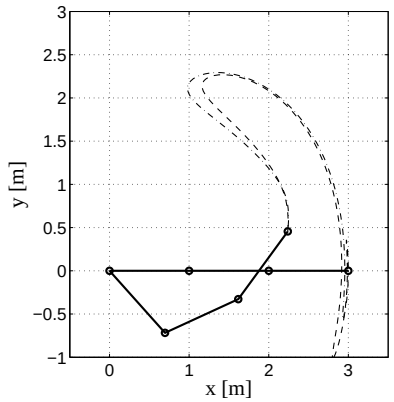

Figure 8. Manipulator's tip path in the task space: original TVO controller (- -), simplified TVO controller (-.-).

than e_3. As a result e_1 converges to zero, but only as a last one (compare remarks from the proof). Orienting process is very effective, which comes directly from Fig. 10 – directions of $\boldsymbol{g}_2^*$ and $\boldsymbol{h}^*$ vector fields coincide after about $1[s]$. This result seems to justify the VFO methodology. Moreover, using simple geometrical interpretation of the VFO methodology and as $\cos\alpha \rightarrow -1$ one can say, that manipulator reaches the reference posture $\boldsymbol{q}_t$ in the manner . According to Fig. 11 it results, that control signals are bounded, with relatively low cost – non-oscillatory behavior of the controlled system during the transient stage. System movement in the task space has been presented in Fig. 12.

5. Conclusions. In this paper two control stabilization strategies for a 3-link nonholonomic manipulator have been presented. Performances of both controllers have been examined by numerical simulations. The first stabilization approach uses a time-varying control law based on the tuned kinematic oscillator concept and ensures practical stability. It can be used to stabilize other underactuated systems such as the unicycle robot, the skid-steering vehicle [12] and others. Moreover, because TVO control signals are time-differentiable, the TVO stabilizer can be easily extended to include dynamic model of the controlled system [4, 12]. The second controller - VFO stabilizer - results from a simple and intuitive geometrical interpretation of the controlled kinematic structure and its possible time evolution in response to specific inputs. This stabilizer belongs to the class of non-Lipschitz continuous controllers guaranteeing asymptotic stability. The VFO stabilizer can be treated as an extension of the tracking controller introduced in [6] and can be applied also to another nonholonomic kinematics with specific structure like unicycle robot, car-like robot or chained system.

References

[1] M. Aicardi, G. Casalino, A. Bicchi, and A. Balestrino. Closed loop steering of unicycle-like vehicles via Lyapunov techniques. *IEEE Robotics and Automation Magazine*, 2:27–35, 1995.

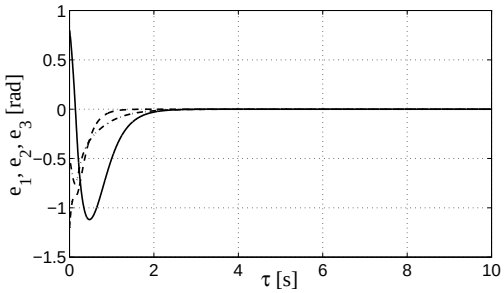

Figure 9. Stabilization errors for VFO controller: $e_1(\tau)$ (–), $e_2(\tau)$ (- -), $e_3(\tau)$ (-.-).

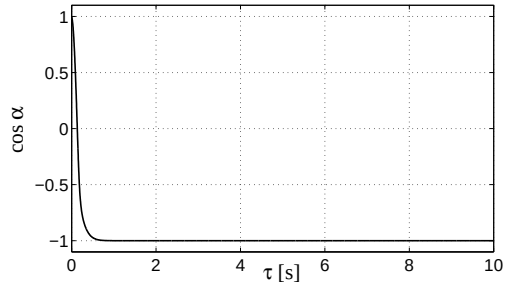

Figure 10. Time plot of $\cos\alpha$, where $\alpha\angle(\boldsymbol{g}_2^*, \boldsymbol{h}^*)$ (VFO controller).

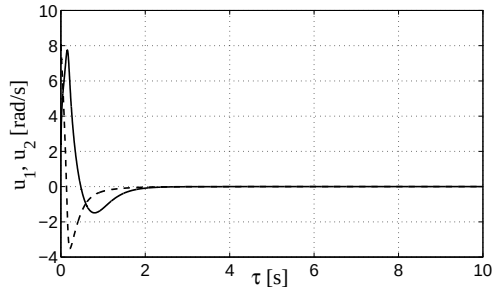

Figure 11. Control signals of VFO controller: orienting control $u_1(\tau)$ (- -) and pushing control $u_2(\tau)$ (–).

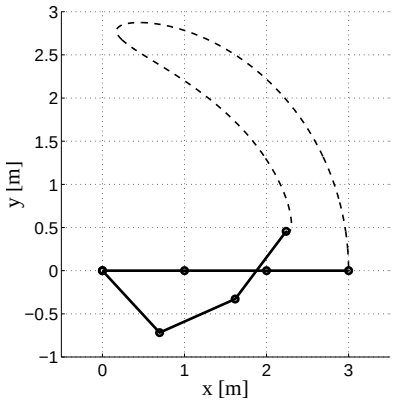

Figure 12. Manipulator's tip path in the task space for VFO controller.

[2] A. Astolfi. *Asymptotic stabilization of nonholonomic systems with discontinuous control*. PhD thesis, Swiss Federal Institute of Technology, Zurich, 1996.

[3] R. W. Brockett. Asymptotic stability and feedback stabilization. In R. W. Brockett, R. S. Millman, and H. H. Sussmann, editors, *Differential Geometric Control Theory*, pages 181–191. Birkhäuser, Boston, 1983.

[4] W. E. Dixon, D. M. Dawson, E. Zergeroglu, and A. Behal. *Nonlinear control of wheeled mobile robots*. Springer, London, 2001.

[5] M. Michałek and K. Kozłowski. Control of nonholonomic mobile robot with vector field orientation (in Polish). *VIII National Robotics Conference (in print)*, 2004.

[6] M. Michałek and K. Kozłowski. Tracking controller with vector field orientation for 3-D nonholonomic manipulator. In *Proceedings of the 4th International Workshop On Robot Motion and Control*, pages 181–189, Puszczykowo, 2004.

[7] I. Kolmanovsky and N. H. McClamroch. Developments in nonholonomic control problems. *IEEE Control Systems Magazine*, 15(6):20–36, 1995.

[8] P. Morin and C. Samson. Field oriented control of induction motors by application of the transverse function control approach. In *42nd IEEE Conference on Decision and Control*, pages 5921–5926, 2003.

[9] P. Morin and C. Samson. Practical stabilization of driftless systems on Lie groups: the transverse function approach. *IEEE Transactions on Automatic Control*, 48(9):1496–1508, September 2003.

[10] P. Morin and C. Samson. Trajectory tracking for nonholonomic vehicles: overview and case study. In *Proceedings of the 4th International Workshop On Robot Motion and Control*, pages 139–153, Puszczykowo, 2004.

[11] Y. Nakamura, W. Chung, and O. J. Sørdalen. Design and control of the nonholonomic manipulator. *IEEE Transactions on Robotics and Automation*, 17(1):48–59, February 2001.

[12] K. Kozłowski and D. Pazderski. Modelling and control of 4-wheel skid-steering mobile robot. *International Journal of Applied Mathematics and Computer Sciences*, 14(4):477–496, 2004.

[13] O. J. Sørdalen, Y. Nakamura, and W. J. Chung. Control of a nonholonomic manipulator. In L. Sciavicco, C. Bonivetto, and F. Nicolo, editors, *Robot Control 1994*, pages 279–284. Pergamon, Capri, Italy, 1994.